Electronic Supplementary Material (ESI) for Journal of Materials Chemistry A.

# Supplementary Information

Tao Feng,[ab] Ying Wang,[ab] Yi-nan Wu,[ab] Daniel Manaye Kabtamu,[abd] Krisztina László,[c] Fengting Li*[ab]

[a] State Key Laboratory of Pollution Control and Resources Reuse, College of Environmental Science and Engineering, Tongji University, Shanghai, 200092, China

[b] Shanghai Institute of Pollution Control and Ecological Security, Shanghai 200092, P.R. China

*mail: fengting@tongji.edu.cn

[c] Department of Physical Chemistry and Materials Science, Budapest University of Technology and Economics, H-1521 Budapest, Hungary

[d] Department of Chemistry, Debre Berhan University, 445, Debre Berhan, Ethiopia

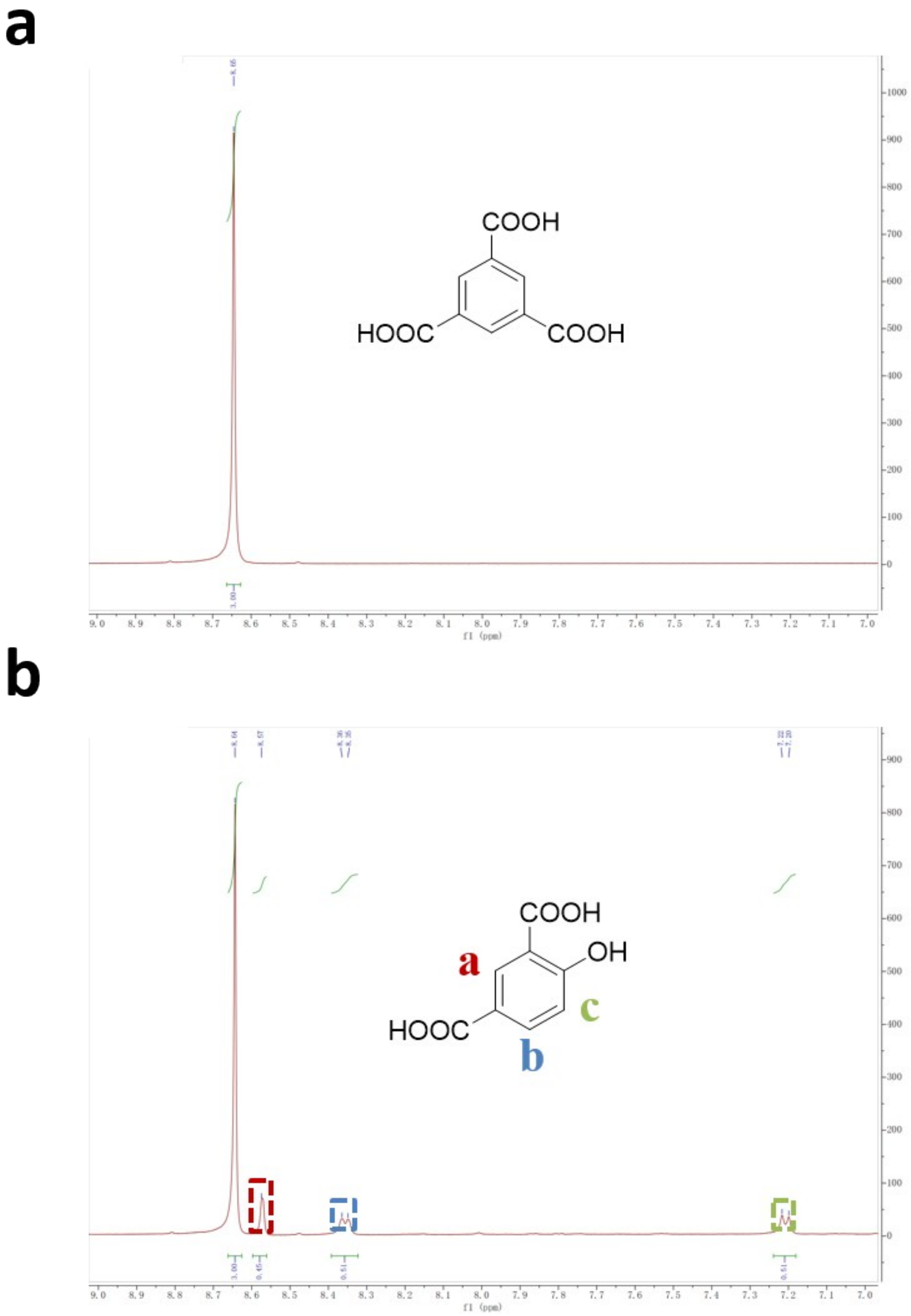

Fig. S1 $^1$H NMR of samples (a) CuBTC and (b) $Cu_2O$@HP-CuBTC (1.5).

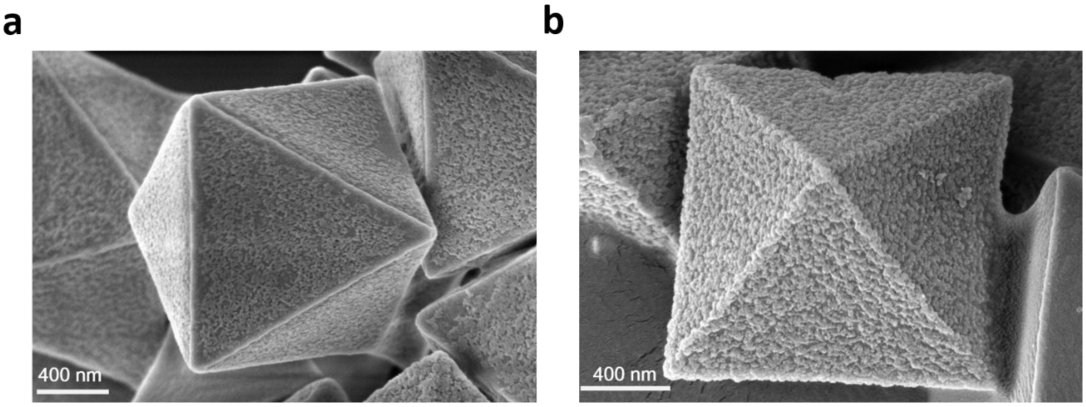

Fig. S2 SEM images of $Cu_2O$@HP-CuBTC (x) (x=1, 2)

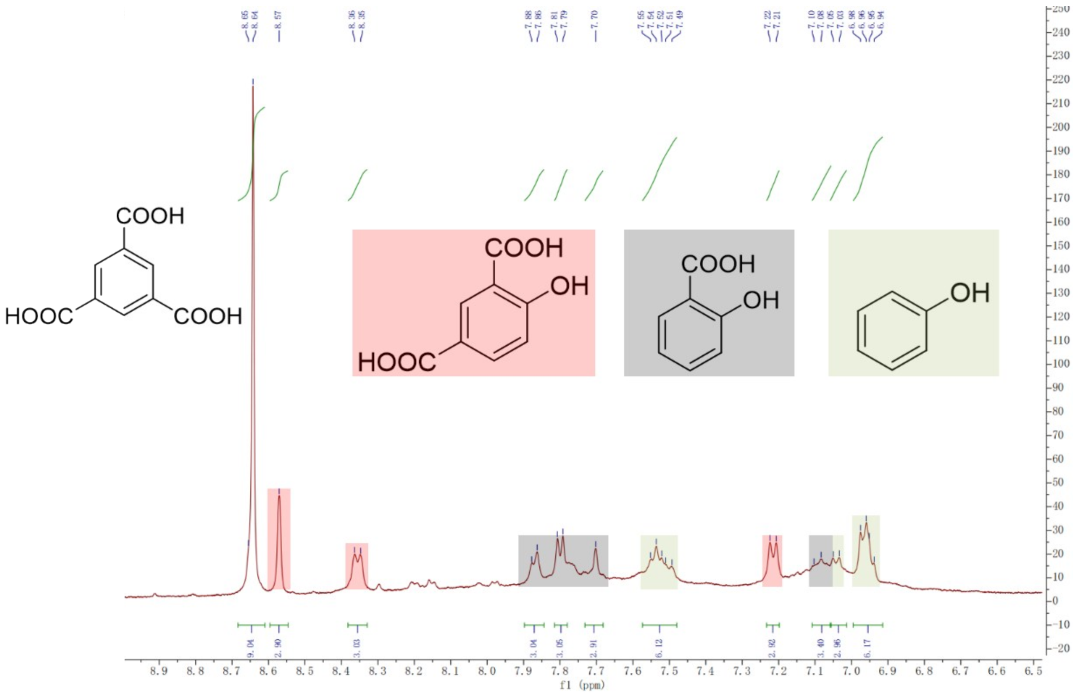

Fig. S3 $^1$H NMR of samples $Cu_2O$@HP-CuBTC (2) solution without washing.

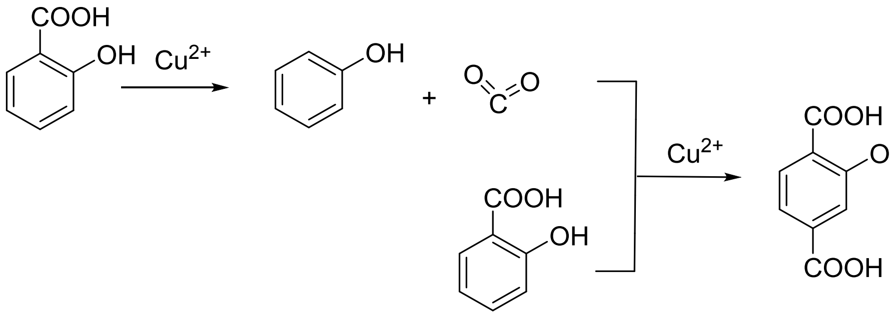

Fig. S4. Composition analysis of $Cu_2O$@HP-CuBTC (x) creation by hydrothermal reaction: L formation equation.

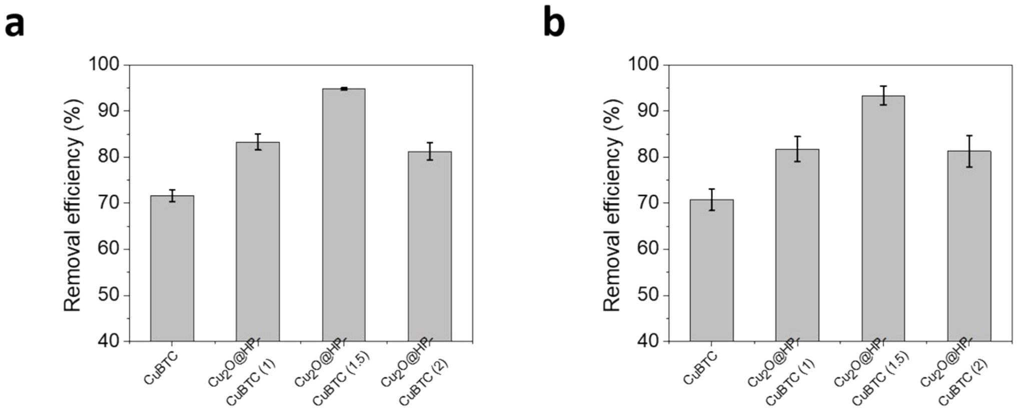

Fig. S5 Removal efficiencies of DBT and BT by CuBTC and $Cu_2O$@HP-CuBTC (x) (x = 1.0, 1.5, 2.0). The initial concentration of (a) DBT and (b) BT are 250 mg-S·$L^{-1}$ for 5h at 298 K.

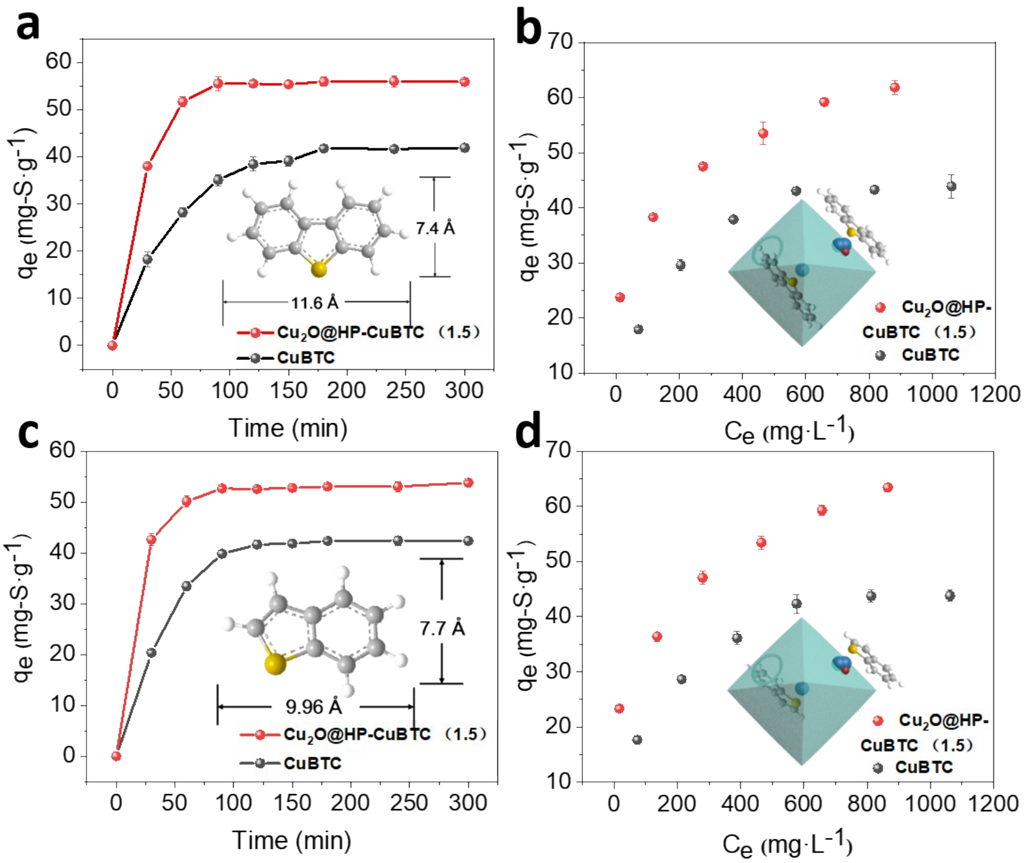

Fig. S6. Comparison of adsorption kinetics and adsorption capacity of $Cu_2O$@HP-CuBTC (1.5) and CuBTC: (a) Effect of contact time on the adsorption capacity with 1000 mg-S·$L^{-1}$ DBT. (b) Effect of the equilibrium concentration of DBT on the adsorption capacity after 5 h. (c) Effect of contact time on the adsorption capacity with 1000 mg-S·$L^{-1}$ BT.(d) Effect of the equilibrium concentration of BT on the adsorption capacity for 5 h at 298 K.

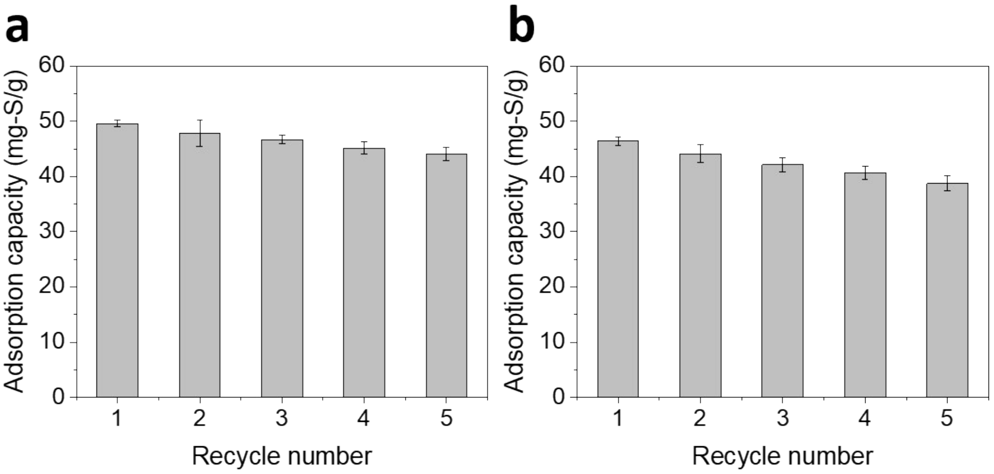

Fig. S7 Cycle-use performance of the $Cu_2O$@HP-CuBTC (1.5) in (a) DBT and (b) BT adsorption with 1000 mg-S·$L^{-1}$ DBT/BT at 298 K.

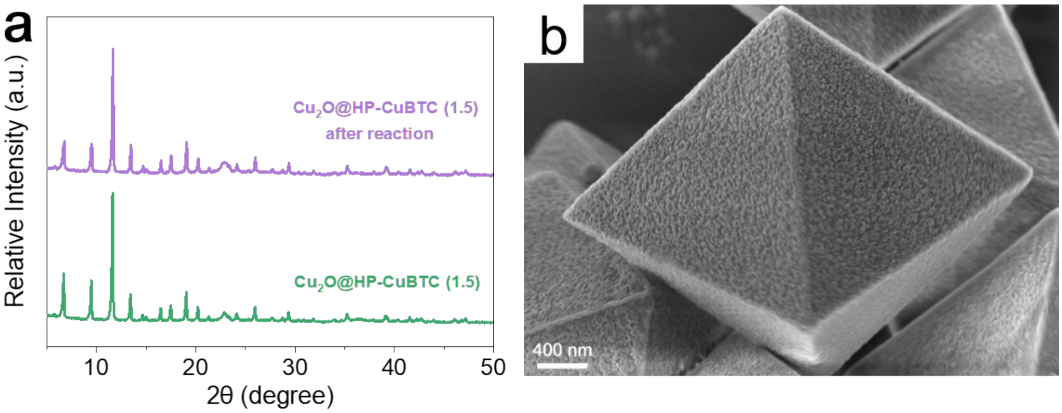

Fig. S8. (a) XRD of $Cu_2O$@HP-CuBTC (1.5) and $Cu_2O$@HP-CuBTC (1.5) after reaction (b) SEM image of $Cu_2O$@HP-CuBTC (1.5) after reaction

The linear form of the Langmuir and Freundlich adsorption isotherm equations are generally expressed as follows:

$$\frac{C_e}{q_e}=\frac{C_e}{q_{max}}+\frac{1}{K_L q_{max}}$$

$$lnq_e = lnK_F + \frac{1}{n}lnC_e$$

Where $C_e$ is the equilibrium concentration of DBT and BT in the solution; $q_e$ is the amount of DBT/BT adsorbed at equilibrium (mg-S·g$^{-1}$), $q_{max}$ and $K_L$ are the theoretical maximum adsorption capacity (mg-S·g$^{-1}$) and Langmuir adsorption equilibrium constant (L·mg$^{-1}$), respectively, and *1/n* and $K_F$ are the heterogeneity factor and Freundlich constant [(mg·g$^{-1}$) (L·mg$^{-1}$)$^{1/n}$], respectively.

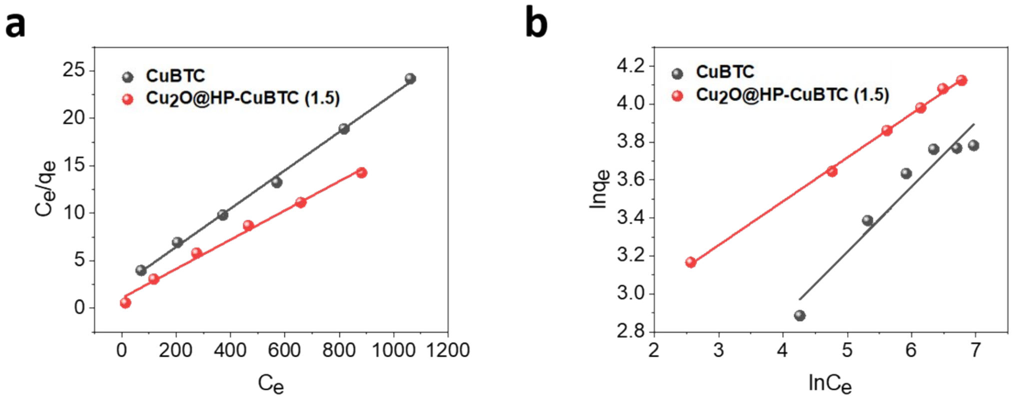

Fig. S9. Adsorption data simulation with (a) Langmuir and (b) Freundlich isotherm adsorption models on $Cu_2O$@HP-CuBTC (1.5) and CuBTC with 250-1500 mg-S·$L^{-1}$ DBT for 5 h at 298 K.

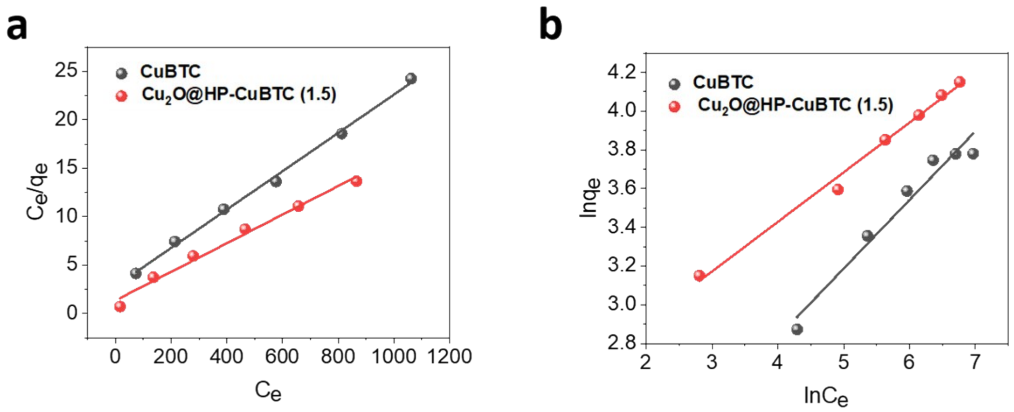

Fig. S10. Adsorption data simulation with (a) Langmuir and (b) Freundlich isotherm adsorption models on $Cu_2O$@HP-CuBTC (1.5) and CuBTC with 250-1500 mg-S·$L^{-1}$ BT for 5 h at 298 K.

Pseudo-first-order kinetic and Pseudo-second-order kinetic are expressed respectively as follows:

$$\ln\left(q_e - q_t\right) = lnq_e - k_1 t$$

$$\frac{t}{q_t} = \frac{1}{k_2 q_e^2} + \frac{t}{q_e}$$

Where $q_t$ (mg-S·g$^{-1}$) is the adsorbed amount of adsorbate at time of $t$ (min) and $q_e$ is the amount of DBT/BT adsorbed at equilibrium (mg-S·g$^{-1}$). $k_1$ and $k_2$ are the pseudo-first-order and pseudo-second-order rate constant (mg·min·g$^{-1}$), respectively.

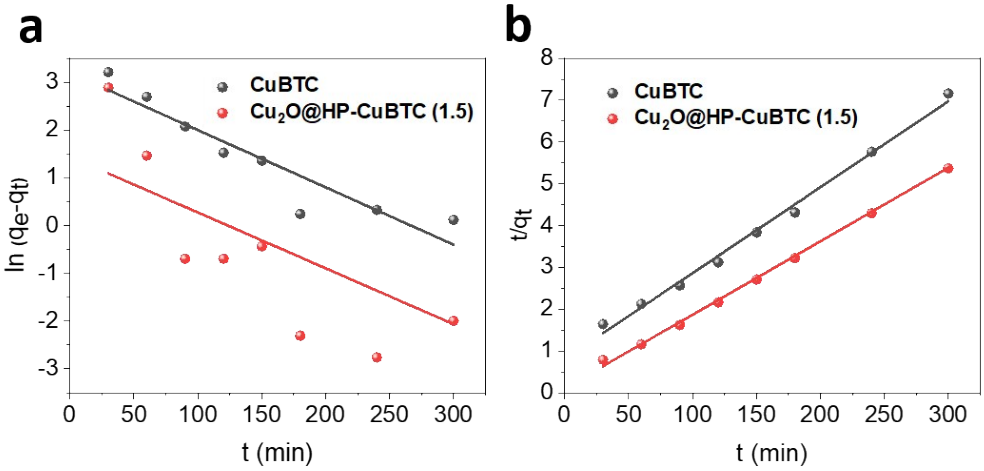

Fig. S11 Adsorption kinetic fitting with (a) pseudo-first-order model and (b) pseudo-second-order model on $Cu_2O$@HP-CuBTC (1.5) and CuBTC with 1000 mg-S·$L^{-1}$DBT at 298 K.

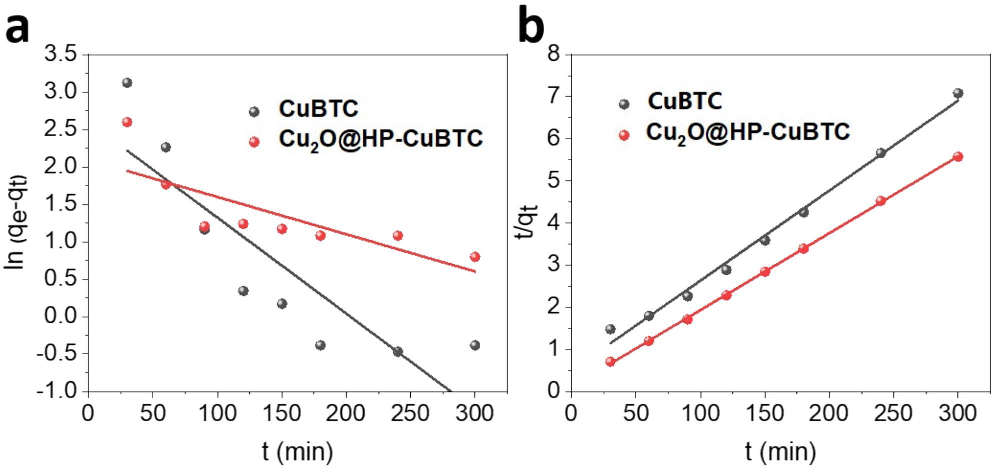

Fig. S12 Adsorption kinetic fitting with (a) pseudo-first-order model and (b) pseudo-second-order model on $Cu_2O$@HP-CuBTC (1.5) and CuBTC with 1000 mg-S·$L^{-1}$ BT at 298 K.

Table S1. Porosity properties of the prepared CuBTC materials

| Sample | $S_{BET}$ ($m^2 \cdot g^{-1}$) | Average Pore diameter (nm) | $V_{micro}$/ $V_{meso}$ |
|---|---|---|---|
| CuBTC | 1198.99 | 1.89 | - |
| $Cu_2O$@HP-CuBTC (1) | 1187.94 | 2.85 | 4.44 |
| $Cu_2O$@HP-CuBTC (1.5) | 1262.15 | 2.91 | 4.29 |
| $Cu_2O$@HP-CuBTC (2) | 1106.29 | 2.93 | 4.18 |

The specific surface area was calculated by employing the Brunauer–Emmett–Teller (BET) method in the range of relative pressure from 0.05 to 0.25. The average pore diameter was determined by the density functional theory method in the adsorption branch of the $N_2$ isotherm at 77 K. Total pore volume was determined using the adsorption branch of the isotherm at $P/P_0 = 0.99$. The mesopore volume ($V_{meso}$) was calculated from Barrett–Joyner–Halenda (BJH) desorption cumulative volume of pores between 1.70 and 300.00 nm diameter. The micropore volume ($V_{micro}$) was obtained by t-plot micropore analysis.

Table S2. Position (eV) and area of C1s region on CuBTC.

| Peak | Position (eV) | Area |
|---|---|---|
| C-O | 286.257 | 3202.401 |
| C-C | 284.803 | 20148.730 |
| O-C=O | 288.2 | 4951.440 |

Table S3. Position (eV) and area of C1s region on $Cu_2O$@HP-CuBTC (1.5).

| Peak | Position (eV) | Area |
|---|---|---|
| C-O | 286.215 | 3198.332 |
| C-C | 284.825 | 20702.900 |
| O-C=O | 288.174 | 4010.424 |

Table S4. Isotherm parameters for adsorption of DBT onto $Cu_2O$@HP-CuBTC (1.5) and CuBTC at 298 K for 5 h

| Adsorption model | Parameter | Sample | |
|---|---|---|---|
| | | $Cu_2O$@HP-CuBTC (1.5) | CuBTC |
| Langmuir | $K_L$ (L mg$^{-1}$) | 0.014 | 0.008 |
| | $q_{max}$ (mg-S g$^{-1}$) | 65.20 | 49.58 |
| | $R^2$ | 0.9956 | 0.9987 |
| Freundlich | $K_F$ | 13.01 | 4.572 |
| | n | 4.338 | 2.936 |
| | $R^2$ | 0.9987 | 0.8348 |

Table S5. Isotherm parameters for adsorption of BT onto $Cu_2O$@HP-CuBTC (1.5) and CuBTC at 298 K for 5 h

| Adsorption isotherm | Parameter | Sample | |
|---|---|---|---|
| | | $Cu_2O$@HP-CuBTC (1.5) | CuBTC |
| Langmuir | $K_L$ (L mg$^{-1}$) | 0.011 | 0.007 |
| | $q_{max}$ (mg-S g$^{-1}$) | 67.71 | 50.56 |
| | $R^2$ | 0.9930 | 0.9983 |
| Freundlich | $K_F$ | 11.07 | 4.119 |
| | n | 3.906 | 2.823 |
| | $R^2$ | 0.9897 | 0.9483 |

Table S6 Kinetic parameters for adsorption onto $Cu_2O$@HP-CuBTC (1.5) and CuBTC with 1000 mg-S·$L^{-1}$ DBT

| Kinetic model | Parameter | Sample | |
|---|---|---|---|
| | | $Cu_2O$@HP-CuBTC (1.5) | CuBTC |
| Pseudo-first-order | $k_1$ (mg min $g^{-1}$) | 0.012 | 0.012 |
| | $q_e$ (mg $g^{-1}$) | 4.235 | 24.48 |
| | $R^2$ | 0.3303 | 0.8794 |
| Pseudo-second-order | $k_2$ (mg min $g^{-1}$) | 0.000034 | 0.000342 |
| | $q_e$ (mg $g^{-1}$) | 56.85 | 48.66 |
| | $R^2$ | 0.9934 | 0.9972 |

Table S7 Kinetic parameters for adsorption onto $Cu_2O$@HP-CuBTC (1.5) and CuBTC with 1000 mg-S·$L^{-1}$ BT

| Kinetic model | Parameter | Sample | |
|---|---|---|---|
| | | $Cu_2O$@HP-CuBTC (1.5) | CuBTC |
| Pseudo-first-order | $k_1$ (mg min $g^{-1}$) | 0.005 | 0.013 |
| | $q_e$ (mg $g^{-1}$) | 8.117 | 13.49 |
| | $R^2$ | 0.6424 | 0.7580 |
| Pseudo-second-order | $k_2$ (mg min $g^{-1}$) | 0.000036 | 0.000228 |
| | $q_e$ (mg $g^{-1}$) | 54.80 | 46.82 |
| | $R^2$ | 0.9916 | 0.9986 |